



In Vitro Evaluation of Antimicrobial and Biofilm-Modulating Effects of Commercial Cranberry (*Vaccinium Macrocarpon*) Extracts Against *Escherichia Coli* and *Staphylococcus Aureus*

Anisa Veledar-Hamalukić,¹ Monia Avdić,¹ Amra Demirović²

Abstract

Background/Aim: Cranberry (*Vaccinium macrocarpon* Ait) extracts are widely recognised for their antimicrobial properties, particularly in preventing urinary tract infections (UTIs). However, their effects on biofilm formation remain underexplored. This study aimed to authenticate commercially available cranberry extracts, quantify their proanthocyanidin (PAC) content and evaluate their antimicrobial and biofilm-modulating effects against *Escherichia coli* and *Staphylococcus aureus*.

Methods: Two commercially available cranberry extracts were analysed using high-performance liquid chromatography (HPLC) to confirm their authenticity based on anthocyanin profiles. PAC content was determined using a modified Bate-Smith method. Antimicrobial activity was assessed via the microbroth dilution method, determining the minimum inhibitory concentration (MIC) for each extract against two *E. coli* and three *S. aureus* strains. Biofilm formation was evaluated using crystal violet staining, with statistical analyses including paired sample t-tests, Friedman's ANOVA and the Durbin-Conover test.

Results: HPLC analysis confirmed that both extracts were derived from the *V. macrocarpon*. PAC content differed significantly between samples ($p < 0.001$), yet MIC values remained consistent at 125 µg/mL for *E. coli* and 250 µg/mL for *S. aureus*. Notably, at concentrations below the MIC, both extracts unexpectedly enhanced bacterial planktonic growth and biofilm formation, likely due to quorum sensing activation. Statistical analyses revealed significant differences in biofilm formation among *S. aureus* strains, while *E. coli* strains showed a more uniform response.

Conclusion: While cranberry extracts exhibit strong antibacterial properties at MIC levels, their ability to stimulate biofilm formation at sub-inhibitory concentrations raises concerns regarding their application. These findings highlight the need for further molecular studies to optimise cranberry-based interventions against biofilm-associated infections.

Key words: *Vaccinium macrocarpon*; Cranberry extract; Proanthocyanidins; Biofilms; Anti-infective agents; Quorum sensing; *Escherichia coli*; *Staphylococcus aureus*.

1. Faculty of Engineering, Natural and Medical Sciences, Department of Genetics and Bioengineering, International Burch University, Sarajevo, Bosnia and Herzegovina.
2. Amsal Pharmaceuticals d.o.o. Sarajevo, Bosnia and Herzegovina.

Citation:

Veledar-Hamalukić A, Avdić M, Demirović A. In vitro evaluation of antimicrobial and biofilm-modulating effects of commercial cranberry (*Vaccinium macrocarpon*) extracts against *Escherichia coli* and *Staphylococcus aureus*. Scr Med. 2025 May-Jun;56(3):395-415.

Corresponding author:

ANISA VELEDAR-HAMALUKIĆ

T: +387 61 502 290

E: anisa.veledar-hamalukic@stu.ibu.edu.ba

Received: 28 February 2025

Revision received: 10 April 2025

Accepted: 10 April 2025

Introduction

The exploration of cranberries' antibacterial and antibiofilm properties represents a promising avenue for addressing the growing challenge of bacterial infections, particularly those involving *E coli* and *S aureus*. Formation of the biofilm allows single-cell organisms to adopt a group-like behaviour which enables the survival in unfavourable surrounding. Once the expression of surface proteins has been changed, bacteria are able to envelop themselves in the self-produced matrix consisting of extracellular polymeric substances (EPS), carbohydrate-binding proteins, fibres and extracellular DNA.¹ A thick biofilm structure traps the water and nutrients needed for bacterial growth. There is constant communication between the changes of biofilm structure and the protein synthesis within the cell. Due to a lack of nutrients, or the abundance of thereof, the activity of bacterial enzymes is changed to adapt to EPS structure. In the highly hydrated surroundings, proteins of the bacteria's surface can form hydrogen bonds with hydrophilic polysaccharides and thus increase the proximity. Tense structure of biofilm facilitates cell-to-cell interaction and DNA exchange. At the same time, biofilm protects the bacteria from dehydration, the influence of oxidising molecules, altered pH and other xenobiotics. The structure of biofilm is rather heterogeneous, with different subpopulations of bacteria with versatile gene expression due to oxygen availability and nutrients.² Such a complex structure is efficient against the antibacterial effect of many antibiotics and is a reason for health concerns. Subpopulations of bacteria in a biofilm can increase the resistance towards antibiotics up to one thousand times stronger compared to a single bacterium. Biofilm also enables the adsorption of molecules to the surface of bacteria, enabling bacterial adhesion to the surface and colony formation.

Bacteria that are most known for forming biofilms include *Pseudomonas aeruginosa*, *Staphylococcus aureus*, *Escherichia coli*, *Staphylococcus epidermidis* and *Bacillus cereus*. There are five stages of biofilm formation: initial reversible attachment, irreversible attachment, maturation (I and II) and dispersion. Depending on the surface surrounding, its pH, concentration of nutrients, ionic forces and temperature and due to Brownian motion and gravity force, bacteria find it suitable to attach to the surface via its flagella, thus

overcoming hydrodynamic and surface tension forces.³ This initial attachment is reversible, because hydrodynamic forces of the surrounding can overcome the flagella adhesion, or bacteria sense the more abundant nutrients are present elsewhere.

The forces influencing bacterial attachment include hydrophobic, steric, electrostatic, van der Waals and protein adhesion. Together, these forces help bacteria stick to surfaces, overcome repulsion and attach permanently, forming a monolayer.⁴ Transition to irreversible attachment is characterised by the reduction of flagella gene expression and increased synthesis of biofilm matrix production. Biofilm maturation involves the formation of cell clusters (maturation stage I), which later develop into microcolonies (maturation stage II).⁵ If the matrix components are degraded, bacteria actively or passively return to their planktonic state, which enables them to spread to new surfaces.

Staphylococcus aureus and *Staphylococcus epidermidis* are significant biofilm-forming bacteria that are associated with surgical device infections. They can produce polysaccharide intracellular adhesin (PIA) that enables them to adhere to medical devices and evade the host immune response. Formed biofilm protects them from the antibiotics and their virulence in the host is enhanced.⁶

Escherichia coli is a Gram-negative bacteria responsible for biofilm formations associated with uroepithelial cell infection.⁷ A variety of microorganisms can cause urinary tract infection (UTI), however, uropathogenic strains of *E coli* (UPEC) are responsible for 80 % of uncomplicated and 65 % of complicated UTIs.⁸

Within the first 6 to 8 hours after infiltrating the cells, UPEC forms intracellular bacterial communities (IBC), that divide rapidly and gather into small clusters. These early IBCs morph into solid biomass. The maturation stage shifts from the early to the middle stage. Each IBC is made of 104 - 105 bacteria and the number of IBCs of the infected bladder can vary from 3 to 700.⁹ Once the IBC enlarges, individual UPEC cells disperse from the structure inside the bladder lumen, where they can re-initiate the process.

Inhibition of bacterial adhesion and biofilm formation is the property of the cranberry proanthocyanins that represents a particular clinical interest. There are two proposed mechanisms of antibiofilm formation, one that is unique to proanthocyanidins A, especially A2, which directly binds to PapGII of *E coli* and prevents its adhesion; and the second one is that components from *V macrocarpon* cause change in gene expression that leads to the increased synthesis of THP (Tamm - Horsfall protein), which naturally enables binding of *E coli* to urethral epithelium by type 1 pili.¹⁰

Proanthocyanidin A2 contains interflavanyl bonds that act like a receptor analogue to a surface of the P-pili of *E coli*. The most favourable conformation of PAC A for the competitive binding to the pili is the trimer form.¹¹ Once bound to the surface of the P pili, PAC A inhibits further agglomeration of the bacteria because they have already interacted with bacteria's hydrophobic motifs and thus, made them more hydrophilic. Since hydrophobicity is a must for a biofilm formation, this auxiliary property further enhances biofilm inhibition.¹²

Proanthocyanidins A1 and A2 are stereoisomers and A1 has more favourable structure of hydroxyl group at position 3 of the pyrene ring to act as a receptor analogue. Proanthocyanidin B contains a single interflavanyl bond between carbon-4 of the B-ring and either C-8 or C-6 of the C-ring. Such structure is not stereochemically favourable for the binding with the galactose disaccharide of the P pili.¹²

Building on the foundation of these insights into biofilm formation and the antimicrobial potential of proanthocyanidins, this study aimed to make an original contribution to the field. By focusing on commercially available dry cranberry extracts, this work investigated their authenticity in terms of *Vaccinium macrocarpon* origin and evaluate their biological properties. Specifically, the study aimed to determine the total proanthocyanidin (PAC) content and assess the minimum inhibitory concentration (MIC) and antibiofilm efficacy of these extracts against *Escherichia coli* and *Staphylococcus aureus*.

Methods

Plant material

Two commercially available dry extracts of *Vaccinium macrocarpon* Aiton. fruit were used in the study. One is Exocyan Cranberry Extract purchased from Nexira™ and the other is extract purchased from Shaanxi Jiahe Phytochem Co, Ltd. To confirm if the purchased extracts were indeed derived from the *V macrocarpon*, the high-performance liquid chromatography (HPLC) method by Brown and Shipley was adjusted and used for screening of the anthocyanins profile.¹³

HPLC instrumentation and chromatographic conditions

An Agilent 1260 Infinity HPLC System (Agilent, USA) was used for the analysis, a quadruple-channel gradient pump, an integrated degasser, an autosampler, a column compartment and a diode array detector were also utilised. Data collection and further processing were done with Agilent OpenLAB CDS ChemStation Edition for LC System. Ingredients were separated on Zorbax C18 5µm 150 x 4.6 mm HPLC Column. Separation of analytes was achieved with gradient elution. Mobile phase A (MPA): water-phosphoric acid (99.5 + 0.5, v/v); mobile phase B (MPB): water-acetonitrile-glacial acetic acid-phosphoric acid (50.0 + 48.5 + 1.0 + 0.5, v/v/v/v). The flow rate and injection volume were 0.9 mL/min and 10 µL, respectively. Experiments were performed at a column and autosampler temperature of 25 °C and detection was performed at 520 nm. About 0.250 g (\pm 0.025 g) of the sample was weighted into a 50 mL conical tube, with 20 mL extraction solvent, sonicated for 45 min, followed by centrifuge at 4500 rpm for 10 min. The supernatant was decanted into a 25 mL volumetric flask and brought to volume with extraction solvent.

Standards were prepared by weighing 10.0 ± 1.0 mg of each standard into separate amber 10 mL volumetric flasks. Approximately 5 mL 2 % (v/v) HCl in methanol solution was added to each flask and sonicated until all solid material dissolved. The flasks were then brought to volume with the addition of 2 % (v/v) HCl in methanol solution. Solutions were stored at 4-8 °C when not in use. Individual stock solutions of each standard were prepared by weighing 10.0 ± 1.0 mg of each standard into separate amber 10 mL volumetric flasks. Then, 5 mL of 2 % (v/v) HCl in methanol was added to each flask. Solutions were sonifi-

cated until dissolved completely and brought to volume with the same solvent. A mixed anthocyanin reference standard solution was prepared by transferring 400 μ L C3Ga stock solution, 100 μ L C3Gl stock solution, 400 μ L C3Ar stock solution, 70 μ L P3Ga stock solution, 30 μ L P3Ar stock solution and 8100 μ L 2 % (v/v) HCl in methanol solution into a test tube. The mixed anthocyanin reference solution was stored at 4-8 °C. A nylon 0.45 μ m filter was used for the mobile phase and for filtering all the prepared solutions.

Chemicals used were:

1. Acetonitrile (CH_3CN). Purity 99.8 % (GC), HPLC grade or equivalent.
2. Methanol (CH_3OH). Purity 99.97 %, HPLC grade or equivalent.
3. Ultrapure water, filtered through Milli-Q Advantage 10, *Merck Millipore Co*, SAD.
4. Hydrochloric acid (HCl in H_2O ; 33–40 %). Purity HPLC grade or equivalent.
5. Glacial acetic acid (CH_3COOH). Purity HPLC grade or equivalent.
6. Phosphoric acid (H_3PO_4 in H_2O ; 55–95 %). Purity HPLC grade or equivalent.
7. Reference standard diluent. Methanol (33–40 %)-HCl (98 + 2, v/v).

Standards were:

1. Cyanidin-3-O-Galactoside Chloride (C3Ga), LGC;
2. Cyanidin-3-O-glucoside (C3Gl), phyproof[®] Reference Substance, *Sigma Aldrich*;
3. Cyanidin-3-O-arabinoside (C3Ar), phyproof[®] Reference Substance, *Sigma Aldrich*;
4. Peonidin-3-O-galactoside (P3Ga), LGC;
5. Peonidin-3-O-arabinoside (P3Ar), Extra-synthesis.

Spectrophotometric determination of total PAC with modified Bate-Smith method

An assay of total PACs was performed by the modified Bate-Smith method using a UV-VIS spectrophotometer Cary 100, *Agilent*, SAD. Reagent: 0.015 g of $\text{Fe}_2(\text{SO}_4)_3$ was mixed with 50 mL HCl 37 % and 50 mL of n-butanol. The reagent is light-sensitive and should be covered with aluminium paper.

Sample preparation. Two tests per sample are performed. 30 mg of sample is weighed into 100 mL vial and filled with MQ water. Tube A contains 2 mL of the sample and 6 mL of reagent medium.

The solution was mixed and then half of the liquid was inserted into screw cap test tube B. Tube B was placed in a Bain-Marie bath at 100 °C for 30 minutes and then cooled for 15 minutes in the dark. The rest of the solution (tube A) was left in the dark. Both sample solutions were then diluted in a ratio of 1:100 before measurement, to maintain the linearity within the range of standard dilution. Blank preparation: 2 mL of distilled water was mixed with 6 mL of reagent and prepared the same way as the sample.

Standard solution preparation. Procyanidin B2 phyproof[®] Reference Substance, *Sigma Aldrich*, was used as standard. Several solutions of different concentrations were prepared (0.01; 0.02; 0.1; 0.15; 0.2 mg/mL). The preparation of the standard was the same as sample preparation.

Result interpretation: the absorbance of tube A and tube B was measured in the spectrophotometer at 550 nm against the blank. The calibration curve is established and the proanthocyanidin concentration of the sample can be obtained in relation to the absorbance of the standard ($y = ax + b$).

Determination of MIC using microbroth dilution method

Bacterial strains. The bacterial strains used in this study were *Escherichia coli* ATCC 14169 (EC1), *Escherichia coli* ATCC 25922 (EC2), *Staphylococcus aureus* ATCC 6538 (SA6), *Staphylococcus aureus* NCTC 12393 (SA1) and *Staphylococcus aureus* ATCC 25923 (SA2). These strains were obtained from recognised international culture collections and maintained under appropriate conditions prior to experimentation.

Preparation of inoculum. Inoculum preparation followed the guidelines outlined by the European Committee on Antimicrobial Susceptibility Testing (EUCAST, 2017). Briefly, overnight bacterial cultures were grown in tryptic soy broth (TSB) and adjusted to a turbidity equivalent to 0.5 McFarland standard using sterile saline solution. This corresponds to a bacterial cell concentration of approximately 1.5×10^8 CFU/mL, as verified by standard plate count methods.

Controls. Pure bacterial cultures prepared at the concentration mentioned above were used as positive controls, while uninoculated TSB served as negative controls to confirm the sterility of the medium and solvents used.

Preparation of test samples. A dry cranberry extract was dissolved in dimethyl sulfoxide (DMSO) to prepare stock solutions with an initial 1 mg/mL concentration. The stock solutions were further serially diluted in a 1:1 ratio in TSB to achieve the desired range of concentrations for testing (1000 µg/mL – 1.95 µg/mL). Each concentration was prepared and tested in triplicate.

Experimental conditions. All assays were conducted in a 96-well microtiter plate format. Wells were inoculated with 100 µL of the prepared bacterial suspension and 100 µL of the test sample solution, yielding a total well volume of 200 µL. Plates were incubated at 35 °C for 18–24 hours under static conditions. Following incubation, growth inhibition was assessed visually, with the minimum inhibitory concentration (MIC) defined as the lowest concentration of cranberry extract that prevented visible bacterial growth. The results were read at 595 nm on an *Agilent BioTek Epoch Microplate Spectrophotometer*.

Biofilm formation assay

Biofilm formation was assessed following a crystal violet staining method. After inoculation and incubation of the 96-well plates under experimental conditions, the plates were washed thor-

oughly with distilled water to remove planktonic cells. The plates were then allowed to air dry. Subsequently, 100 µL of 0.1 % (w/v) crystal violet solution was added to each well and incubated for 10 minutes at room temperature. Excess stain was removed by washing the plates again with distilled water, followed by air-drying. To quantify the biofilm, 100 µL of 6 % ethanol was added to each well and incubated for 10 minutes to dissolve the crystal violet bound to the biofilm. The optical density (OD) was recorded at 595 nm using an ELISA plate reader.

Calculation of OD and biofilm classification was performed via MS Excel and used for assessing the adherence of the bacteria to the biofilm. The OD value is calculated according to the formula $3 \text{ STDEV} + \text{Mean OD negative control}$. The interpretation of the biofilm production is performed via the following:

- $\text{OD} \leq \text{ODc}$ = no biofilm producer;
- $\text{ODc} < \text{OD} \leq 2 \times \text{ODc}$ = weak biofilm producer;
- $2 \times \text{ODc} < \text{OD} \leq 4 \times \text{ODc}$ = moderate biofilm producer;
- $4 \times \text{ODc} < \text{OD}$ = strong biofilm producer.¹⁴

Statistical analysis of the results was performed using the *Jamovi* 2.6.24.0 program.

Results

Since the peaks of five anthocyanins characteristic for *V macrocarpon* have matched the retention time of the corresponding standards (Figure 1),

the HPLC method has confirmed that two commercially available extracts used in research were indeed of cranberry origin (Figures 2 and 3).

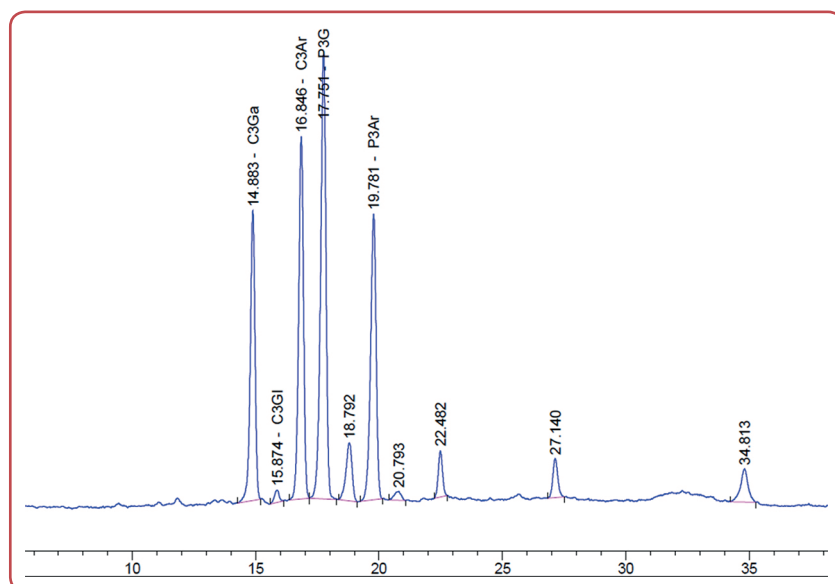


Figure 1: Chromatogram of anthocyanin reference standard solution

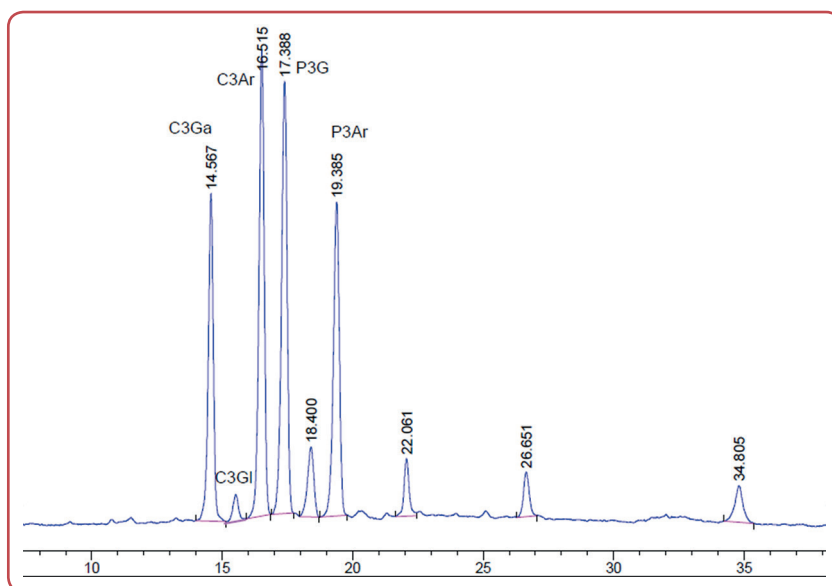


Figure 2: Chromatogram of sample 1 (dry cranberry extract, Nexira™)

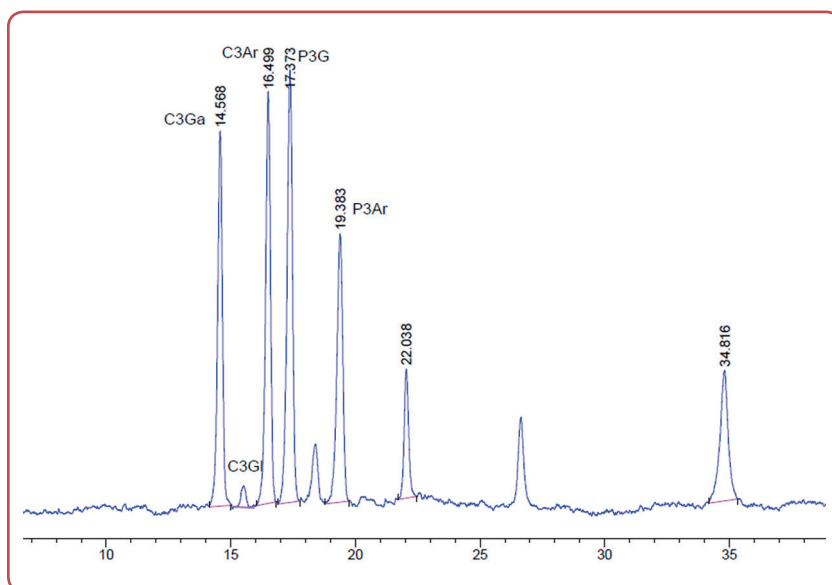


Figure 3: Chromatogram of sample 2 (dry cranberry extract, Shaanxi Jiahe Phytochem Co, Ltd)

Brown and Shipley's method states that the expected order of elution is C3Ga (15.8–15.9 min), C3Gl (16.7–16.9 min), C3Ar (17.7–17.9 min), P3Ga (18.3–18.5 min) and P3Ar (20.2–20.4 min). The relative retention times of the anthocyanin peaks in all solutions are comparable.

Results of total proanthocyanidin content using the modified Bate – Smith method

Proanthocyanidins in diluted mineral acids are cleaved into the carbocation unit (extension units) and the terminal flavan-3-ol unit. The carbocation unit undergoes autooxidation catalysed by Fe (III) sulphate and form corresponding anthocyanidins. Thus, colourless proanthocyanidins convert to red anthocyanidins. The absorbance is measured (max) at ~ 550 nm.

A calibration curve was constructed using pro-cyanidin B2 as the standard, with concentrations ranging from 0.01 – 0.20 mg/mL. The absorbance of the samples and standards was measured at 550 nm and the PAC concentration in each sample was calculated from the calibration curve (Figure 4). The results of total PAC content ($\mu\text{g/mL}$) in two samples are shown in Table 1.

Results of MIC using microbroth dilution method Both cranberry extracts have shown antimicrobial properties. MIC has been determined and shown in Table 2.

It can be observed that for the same strains of bacteria, in the cases of both sample, MIC has same value, in the range of 125 μg for *E coli* strains and 250 μg for *S aureus* strains.

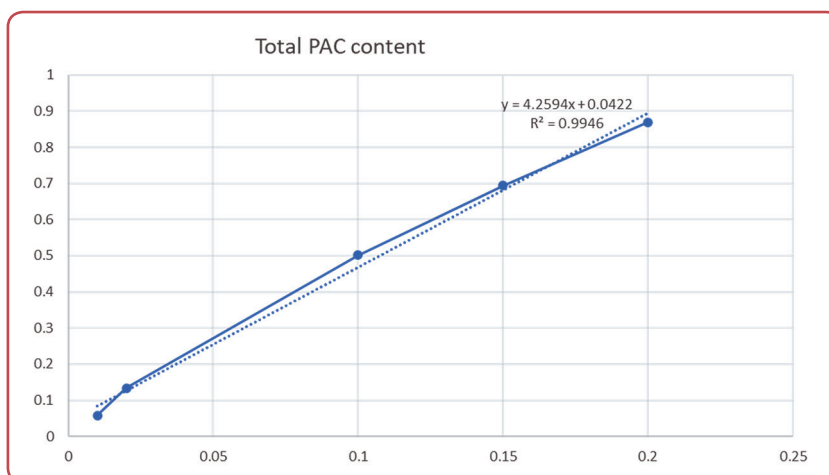


Figure 4: Calibration curve of procyanidin B2 standard

PAC - proanthocyanidin;

Table 1: Results of total proanthocyanidin (PAC) content in sample 1 and 2

No repetitions	Concentration of total PAC (µg/mL), Nexira cranberry (sample 1)	Concentration of total PAC (µg/mL), Shaanxi Jiahe Phytochem Co, Ltd cranberry (sample 2)
Repetition 1	66.163	71.560
Repetition 2	67.356	71.428
Repetition 3	67.382	72.054
Average	66.967	71.681

Based on the results shown in tables (Tables 3 – 7), it can be observed that the samples in question do enhance the planktonic growth of bacteria.

Results of the biofilm formation of sample 1 and 2

The biofilm formation of *E coli* ATCC 14169 for sample 1 (abbreviated as EC1(1)) is presented in Table 8 and Figure 5. Sample 1 was diluted to concentrations ranging from 1000 µg/ml to 1.95 µg/mL. It can be observed that when the sample concentration falls below the MIC, biofilm formation was stimulated.

Table 2: The minimum inhibitory concentration (MIC) of two different dry cranberry extracts on stated bacteria strains

Bacterial strain	<i>E coli</i> ATCC 14169	<i>E coli</i> ATCC 25922	<i>S aureus</i> NCTC 12393	<i>S aureus</i> ATCC 25923	<i>S aureus</i> ATCC 658
MIC: sample 1 (dry cranberry extract Nexira)	125 µg/mL	125 µg/mL	250 µg/mL	250 µg/mL	250 µg/mL
MIC: sample 2 (Shaanxi Jiahe Phytochem Co, Ltd)	125 µg/mL	125 µg/mL	250 µg/mL	250 µg/mL	250 µg/mL

Table 3: The minimum inhibitory concentration (MIC) of dry cranberry extract, sample 1 on *E coli* ATCC 14169, EC1(1) and sample 2 EC1(2) and indicated planktonic growth

Samples	Type of control		Concentration (µg/mL)									
	Negative	Positive: <i>E coli</i> ATCC 14169	1000	500	250	125	62.5	31.25	15.63	7.81	3.91	1.95
	1	2	3	4	5	6	7	8	9	10	11	12
EC1(1)	0.054	1.414	0.184	0.085	0.113	0.091	0.194	1.485	1.541	1.304	1.647	1.526
EC1(2)	0.057	1.339	0.152	0.098	0.076	0.085	0.209	1.418	1.381	1.466	1.550	1.351



Table 4: The minimum inhibitory concentration (MIC) of dry cranberry extract, sample 1 on *E coli* ATCC 25922, EC2(1) and sample 2 EC2(2) and indicated planktonic growth

Samples	Type of control		Concentration (µg/mL)									
	Negative	Positive: <i>E coli</i> ATCC 25922	1000	500	250	125	62.5	31.25	15.63	7.81	3.91	1.95
	1	2	3	4	5	6	7	8	9	10	11	12
EC1(1)	0.056	1.122	0.171	0.087	0.082	0.123	0.693	1.153	1.296	1.285	1.190	1.002
EC1(2)	0.057	1.204	0.159	0.095	0.086	0.142	0.738	1.251	1.221	1.312	1.296	1.056

Table 5: The minimum inhibitory concentration (MIC) of d62.5ry cranberry extract, sample 1 on *S aureus* NCTC 12393, SA1(1) and sample 2 SA1(2) and indicated planktonic growth

Samples	Type of control		Concentration (µg/mL)									
	Negative	Positive: <i>S aureus</i> NCTC 12393	1000	500	250	125	62.5	31.25	15.63	7.81	3.91	1.95
	1	2	3	4	5	6	7	8	9	10	11	12
SA1(1)	0.057	0.583	0.186	0.099	0.118	0.236	0.350	0.404	0.428	0.867	0.443	0.467
SA1(2)	0.056	0.573	0.161	0.105	0.122	0.274	0.359	0.414	0.402	0.444	0.438	0.594
C	0.063	0.591	0.141	0.167	0.100	0.256	0.355	0.417	0.795	0.410	0.473	0.578

Table 6: The minimum inhibitory concentration (MIC) of dry cranberry extract, sample 1 on *S aureus* ATCC 25923, SA2(1) and sample 2 SA2(2) and indicated planktonic growth

Samples	Type of control		Concentration (µg/mL)									
	Negative	Positive: <i>S aureus</i> ATCC 25923	1000	500	250	125	62.5	31.25	15.63	7.81	3.91	1.95
	1	2	3	4	5	6	7	8	9	10	11	12
SA2(1)	0.055	1.555	0.146	0.088	0.093	0.347	0.678	0.584	0.808	1.135	1.187	1.352
SA2(2)	0.062	1.602	0.145	0.082	0.119	0.599	0.536	0.544	1.016	1.181	1.674	1.491

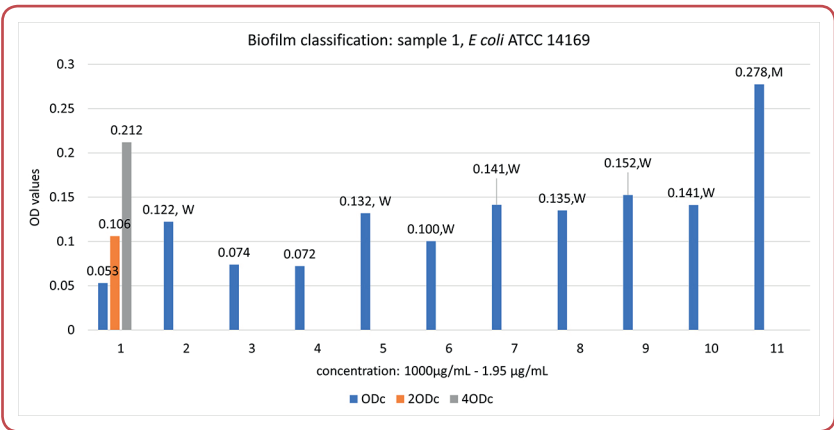
Table 7: The minimum inhibitory concentration (MIC) of dry cranberry extract, sample 1 on *S aureus* ATCC 6538, SA6(1) and sample 2 SA6(2) and indicated planktonic growth

Samples	Type of control		Concentration (µg/mL)									
	Negative	Positive: <i>S aureus</i> ATCC 6538	1000	500	250	125	62.5	31.25	15.63	7.81	3.91	1.95
	1	2	3	4	5	6	7	8	9	10	11	12
SA6(1)	0.056	0.761	0.232	0.086	0.115	0.299	0.663	0.622	0.755	0.882	0.822	0.815
SA6(2)	0.055	0.745	0.155	0.085	0.122	0.350	0.517	0.540	0.579	0.796	0.709	0.714

When same bacteria (EC1) were treated with sample 2, even stronger biofilm formation is noticed, once the concentration is below MIC (Table 9, Figure 6).

When a different strain of *E coli* is treated with solution of sample 1 with concentrations ranging 1000 µg/mL – 1.95 µg/mL, even stronger biofilm formation activity is observed than in EC1(1), as shown in Table 10 and Figure 7.

Figure 5: Sample 1 and the increase of biofilm formation once the concentration was below the minimum inhibitory concentration (MIC), EC1(1)



OD - optical density;

Table 8: Biofilm classification of sample 1 within range of concentrations: 1000 µg/mL – 1.95 µg/mL

Sample 1: E. coli ATCC 14169 EC1(1)	Concentration (µg/mL)									
	1000	500	250	125	62.5	31.25	15.63	7.81	3.91	1.95
ODc	0.081									
2ODc	0.162	0.122	0.074	0.072	0.132	0.100	0.141	0.135	0.152	0.141
4ODc	0.324									
Biofilm classification	W	NA	NA	W	W	W	W	W	W	M

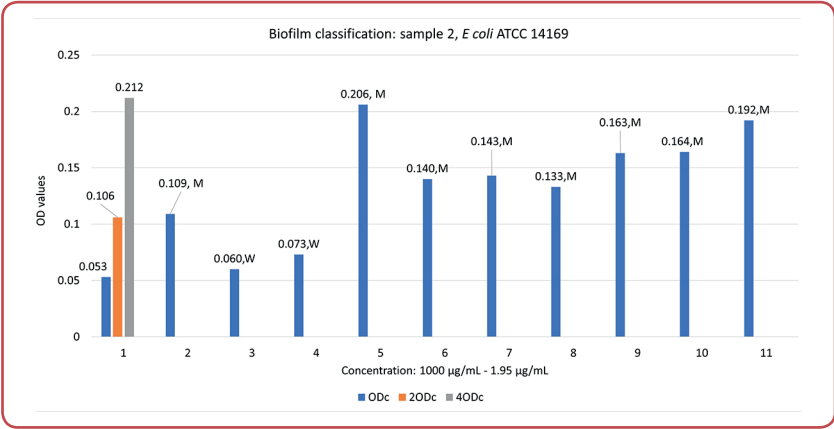
NA – non-adherent; W – weakly adherent; M – moderately adherent; EC1(1); OD - optical density;

Table 9: Biofilm classification of sample 2 within the range of concentrations: 1000 µg/mL – 1.95 µg/mL

Sample 1: E. coli ATCC 14169 EC1(2)	Concentration (µg/mL)									
	1000	500	250	125	62.50	31.25	15.63	7.81	3.91	1.95
ODc	0.053									
2ODc	0.106	0.109	0.060	0.073	0.206	0.140	0.143	0.133	0.163	0.164
4ODc	0.212									
Biofilm classification	M	W	W	M	M	M	M	M	M	M

W – weakly adherent; M – moderately adherent; EC1(2); OD - optical density;

Figure 6: Sample 2 and the increase of biofilm formation once the concentration was below the minimum inhibitory concentration (MIC), EC1(2)



OD - optical density;

Table 10: Biofilm classification of the sample 1 within range of concentrations: 1000 µg/mL – 1.95 µg/mL

Sample 1: <i>E coli</i> ATCC 25922 EC2(1)		Concentration (µg/mL)									
		1000	500	250	125	62.50	31.25	15.63	7.81	3.91	1.95
ODc	0.065										
20Dc	0.130	0.166	0.084	0.087	0.133	0.389	0.330	0.274	0.212	0.212	0.114
40Dc	0.260										
Biofilm classification		M	W	W	M	S	S	S	M	M	W

W – weakly adherent; M – moderately adherent; S- strongly adherent; EC2(1); OD - optical density;

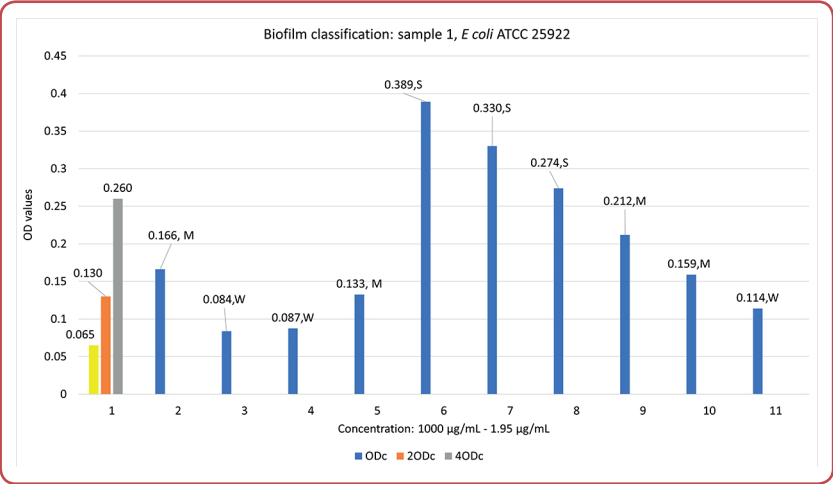


Figure 7: Sample 2 and the increase of biofilm formation once the concentration was below the minimum inhibitory concentration (MIC), EC1(2)

OD - optical density;

Table 11: Biofilm classification of the sample 2 within range of concentrations: 1000 µg/mL – 1.95 µg/mL

Sample 1: <i>E coli</i> ATCC 25922 EC2(2)		Concentration (µg/mL)									
		1000	500	250	125	62.50	31.25	15.63	7.81	3.91	1.95
ODc	0.056										
20Dc	0.112	0.100	0.055	0.090	0.158	0.255	0.201	0.158	0.179	0.145	0.084
40Dc	0.224										
Biofilm classification		W	NA	W	M	S	M	M	M	M	W

NA – non-adherent; W – weakly adherent; M – moderately adherent; S- strongly adherent; EC2(2); OD - optical density;

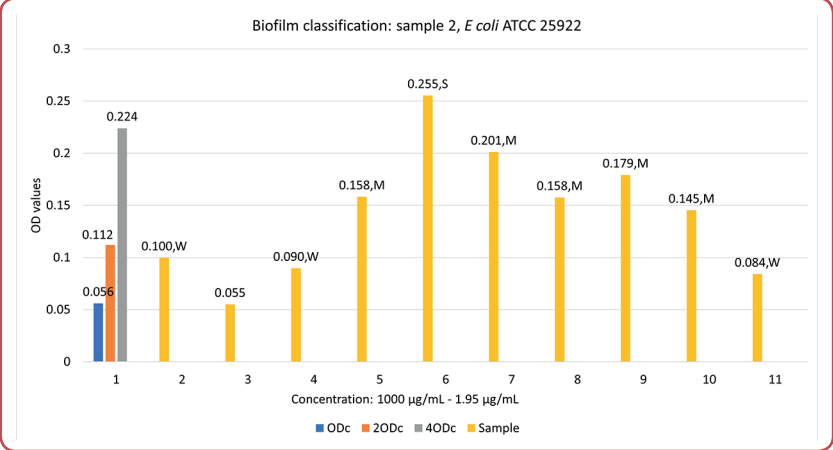


Figure 8: Sample 2 and the increase of biofilm formation once the concentration was below the minimum inhibitory concentration (MIC), EC2(2)

OD - optical density;

Also, the same observation is observed when same *E coli* strain EC2 is treated with sample 2 (Table 11). Tendency to increase biofilm formation is shown at the Figure 8 for EC2(2).

The same experiment was performed on three different strains of *S aureus*: *S aureus* NCTC 12393 - SA1, *S aureus* ATCC 25923 - SA2 and *S aureus* ATCC 6538 - SA6.

As shown in Tables 12, 14, 16, 18, 20 and 22 significant biofilm formation is present in all three strains, when treated with samples within the concentration range of 1000 µg/mL – 1,95 µg/mL.

Because there is moderate to strong adherence in all three cases when treated with both samples, even further dilution has been made and biofilm formation is observed. It needs to be noted that the maximum OD that is measured by the spectrophotometer is 3.000. Overflow value indicates strong adherence of the biofilm. Unexpectedly, even within the range of concentrations of 0.975 µg/mL – 0.0005 µg/mL, biofilm formation was still present (Tables 13, 15, 17, 19, 21 and 23).

Biofilm adherence for all three *S aureus* strains treated with two samples, in concentrations 0.975 µg/mL – 0.0005 µg/mL is shown in Figures 9-14.

Table 12: Biofilm classification SA1(1): 1000 µg/mL – 1.95 µg/mL

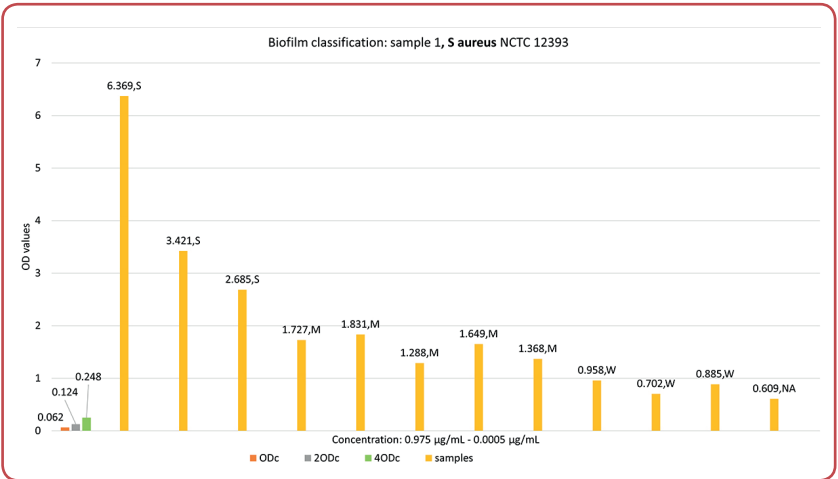
Sample 1	Negative control	Positive control	Concentration (µg/mL)									
			1000	500	250	125	62.50	31.25	15.63	7.81	3.91	1.95
<i>S aureus</i> NCTC 12393 SA1(1)	0.050	0.094	0.083	0.058	0.059	OVRFLW	OVRFLW	OVRFLW	1.769	1.550	2.655	1.466

Table 13: Biofilm classification SA1(1): 0.975 µg/mL – 0.0005 µg/mL

Sample 2: <i>S aureus</i> NCTD 12393 SA1(1)		Concentration (µg/mL)											
		0.975	0.488	0.244	0.122	0.061	0.030	0.152	0.008	0.004	0.002	0.001	0.0005
ODc	0.062												
20Dc	0.124	6.369	3.421	2.685	1.727	1.831	1.288	1.649	1.368	0.958	0.702	0.885	0.609
40Dc	0.248												
Samples		S	S	S	M	M	M	M	M	W	W	W	NA

NA – non-adherent; W – weakly adherent; M – moderately adherent; S - strongly adherent; SA1(1);

Figure 9: Sample 1 and the increase of biofilm formation once the concentration is below the minimum inhibitory concentration (MIC), SA1(1)



OD - optical density;

Table 14: Biofilm classification SA1(2): 1000 µg/mL – 1.95 µg/mL

Sample 2	Negative control	Positive control	Concentration (µg/mL)									
			1000	500	250	125	62.50	31.25	15.63	7.81	3.91	1.95
<i>S aureus</i> NCTC 12393 SA1(2)	0.047	0.204	0.070	0.055	0.074	OVRFLW	OVRFLW	OVRFLW	OVRFLW	OVRFLW	2.987	2.337

Table 15: Biofilm classification SA1(2): 0.975 µg/mL – 0.0005 µg/mL

Sample 2: <i>S aureus</i> NCTD 12393 SA1(2)		Concentration (µg/mL)											
		0.9750	0.4875	0.2440	0.1220	0.0610	0.0300	0.1520	0.0080	0.0040	0.0020	0.0010	0.0005
ODc	0.845												
20Dc	1.690	2.762	1.820	0.966	2.452	0.395	1.255	0.481	2.000	2.671	1.259	1.238	1.385
40Dc	3.380												
Samples		M	M	M	M	NA	W	W	M	M	M	M	M

NA – non-adherent; W – weakly adherent; M – moderately adherent; SA1(2); OD - optical density;

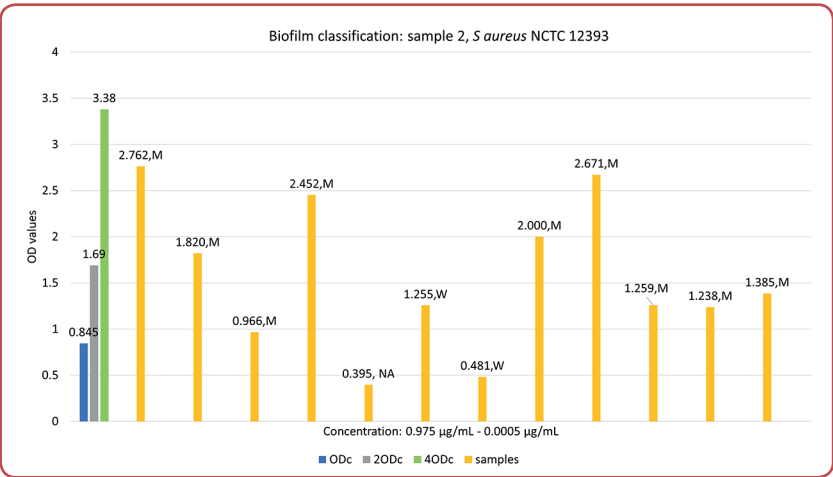


Figure 10: Sample 2 and the increase of biofilm formation once the concentration was below the minimum inhibitory concentration (MIC), SA1(2)

OD - optical density;

Table 16: Biofilm classification SA2(1): 1000 µg/mL – 1.95 µg/mL

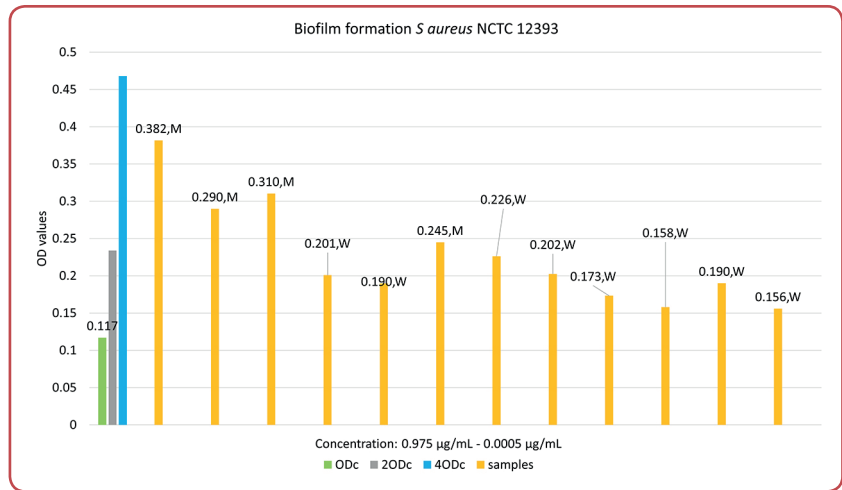
Sample 1	Negative control	Positive control	Concentration (µg/mL)									
			1000	500	250	125	62.50	31.25	15.63	7.81	3.91	1.95
<i>S aureus</i> ATCC 25923, SA2(1)	0.095	0.274	0.087	0.057	0.081	OVRFLW	OVRFLW	0.407	0.162	0.189	0.192	0.162

Table 17: Biofilm classification SA2(1): 0.975 µg/mL – 0.0005 µg/mL

Sample 1: <i>S aureus</i> ATCC 25923, SA2(1)		Concentration (µg/mL)											
		0.9750	0.4875	0.2440	0.1220	0.0610	0.0300	0.1520	0.0080	0.0040	0.0020	0.0010	0.0005
ODc	0.117												
20Dc	0.234	0.382	0.290	0.310	0.201	0.190	0.245	0.226	0.202	0.173	0.158	0.190	0.156
40Dc	0.468												
Samples		M	M	M	W	W	M	W	W	W	W	W	W

W – weakly adherent; M – moderately adherent; SA2(1); OD - optical density;

Figure 11: Sample 1 and the increase of biofilm formation once the concentration was below the minimum inhibitory concentration (MIC), SA2(1)



OD - optical density;

Table 18: Biofilm classification SA2(2): 1000 µg/mL – 1.95 µg/mL

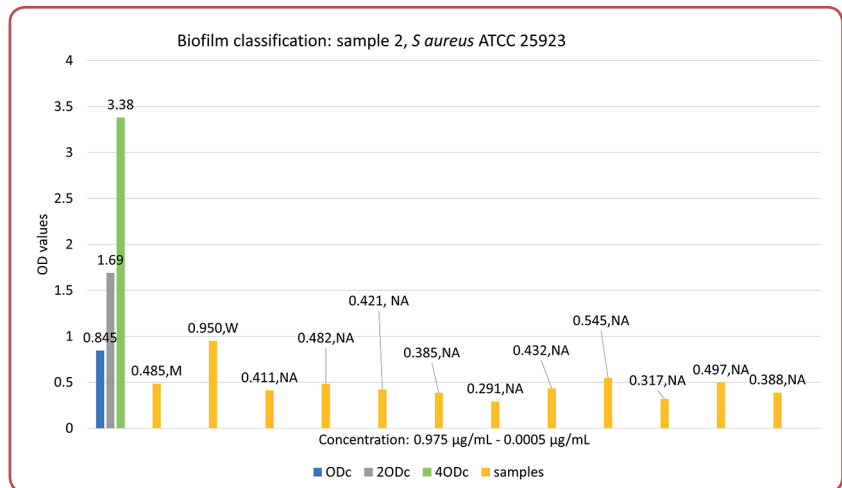
Sample 2	Negative control	Positive control	Concentration (µg/mL)									
			1000	500	250	125	62.50	31.25	15.63	7.81	3.91	1.95
<i>S aureus</i> ATCC 25923, SA2(2)	0.049	0.389	0.068	0.067	0.178	OVRFLW	1.640	0.331	0.316	0.304	0.344	0.388

Table 19: Biofilm classification SA2(2): 0.975 µg/mL – 0.0005 µg/mL

Sample 1: <i>S aureus</i> ATCC 25923, SA2(2)		Concentration (µg/mL)											
		0.9750	0.4875	0.2440	0.1220	0.0610	0.0300	0.0150	0.0075	0.00375	0.001875	0.0009375	0.00046875
ODc	0.845												
2ODc	1.690	0.485	0.950	0.411	0.482	0.421	0.385	0.291	0.432	0.545	0.317	0.497	0.388
4ODc	3.380												
Samples		NA	W	NA	NA	NA	NA	NA	NA	NA	NA	NA	NA

NA – non-adherent; W – weakly adherent; SA2(2);

Figure 12: Sample 2 and the increase of biofilm formation once the concentration was below the minimum inhibitory concentration (MIC), SA2(2)



OD - optical density;

Table 20: Biofilm classification SA6(1): 1000 µg/mL – 1.95 µg/mL

Sample 1: <i>S aureus</i> ATCC 6538, SA6(1)	Concentration (µg/mL)									
	1000	500	250	125	62.50	31.25	15.63	7.81	3.91	1.95
ODc 0.081										
20Dc 0.162	0.132	0.079	0.088	3.660	0.360	0.696	0.308	0.334	0.318	0.219
40Dc 0.324										
Samples	W	NA	W	S	S	S	M	S	M	M

NA – non-adherent; W – weakly adherent; M – moderately adherent; S - strongly adherent; SA6(1); OD - optical density;

Table 21: Biofilm classification SA6(1): 0.975 µg/mL – 0.0005 µg/mL

Sample 1: <i>S aureus</i> ATCC 6538, SA6(1)		Concentration (µg/mL)											
		0.9750	0.4875	0.2440	0.1220	0.0610	0.0300	0.1520	0.0080	0.0040	0.0020	0.0010	0.0005
ODc	0.081												
20Dc	0.162	0.337	0.319	0.242	0.382	0.304	0.378	0.395	0.249	0.336	0.253	0.250	0.191
40Dc	0.324												
Samples		S	M	M	S	M	S	S	M	S	M	M	M

W – weakly adherent; M – moderately adherent; S - strongly adherent; SA6(1); OD - optical density;

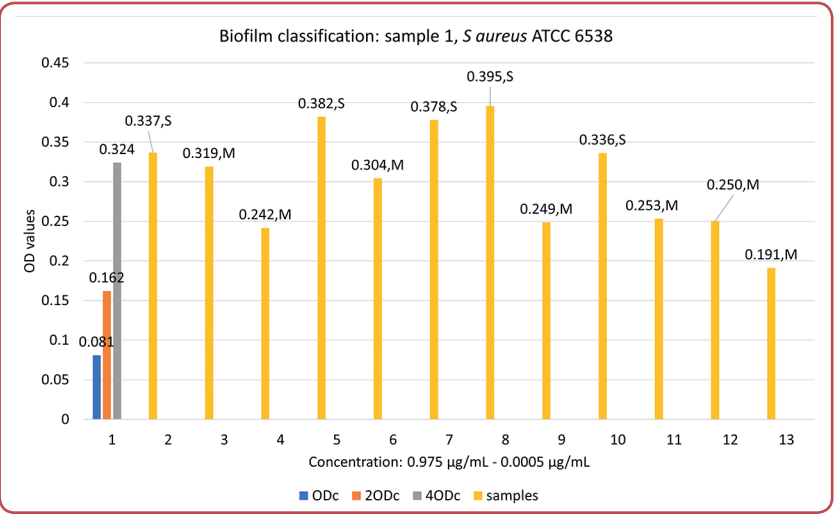


Figure 13: Sample 1 and the increase of biofilm formation once the concentration was below the minimum inhibitory concentration (MIC), SA6(1)

OD - optical density;

Table 22: Biofilm classification SA6(2): 1000 µg/mL – 1.95 µg/mL

Sample 2: <i>S aureus</i> ATCC 6538, SA6(2)	Concentration (µg/mL)									
	1000	500	250	125	62.50	31.25	15.63	7.81	3.91	1.95
ODc 0.081										
20Dc 0.162	0.099	0.065	0.115	2.209	0.635	1.220	0.888	0.492	0.320	0.352
40Dc 0.324										
Samples	W	W	W	M	S	S	S	S	M	S

W – weakly adherent; M – moderately adherent; S - strongly adherent; SA6(2); OD - optical density;

Table 23: Biofilm classification SA6(2): 0.975 µg/mL – 0.0005 µg/mL

Sample 2: <i>S aureus</i> ATCC 6538, SA6(2)		Concentration (µg/mL)											
		0.9750	0.4875	0.2440	0.1220	0.0610	0.0300	0.1520	0.0080	0.0040	0.0020	0.0010	0.0005
ODc	0.069												
20Dc	0.138	1.219	1.463	1.277	0.958	0.938	1.724	0.640	0.459	0.649	0.417	0.367	0.341
40Dc	0.276												
Samples		M	S	S	S	S	S	S	S	S	S	S	S

M – moderately adherent; S - strongly adherent; SA6(2); OD - optical density;

Table 24: Friedman test followed by Durbin-Conover test (cranberry sample 1 tested on 3 strains of *S aureus* within mentioned range of concentration)

ANOVA (Non parametric)	Statistic	p-value
OD <i>S aureus</i> ATCC 6538 - OD <i>S aureus</i> ATCC 25923	3.67	0.001
OD <i>S aureus</i> ATCC 6538 - OD <i>S aureus</i> NCTC 12393	4.90	< 0.001
OD <i>S aureus</i> ATCC 25923 - OD <i>S aureus</i> NCTC 12393	8.57	< 0.001

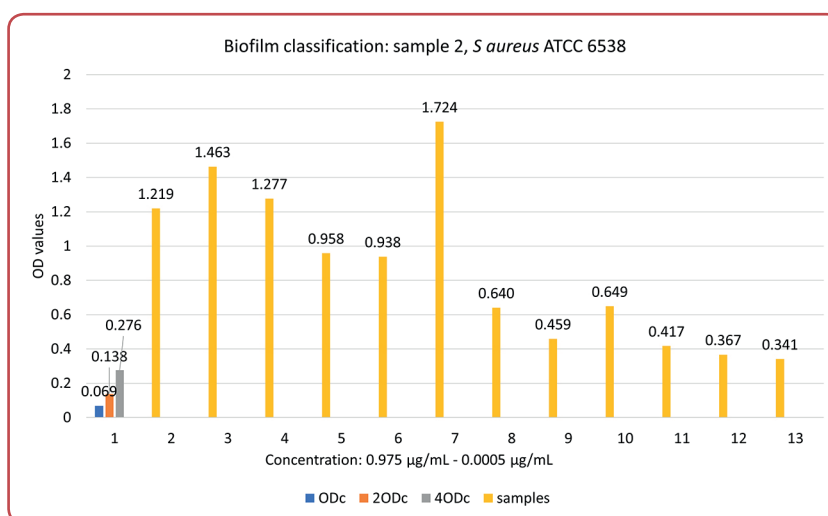


Figure 14: Sample 1 and the increase of biofilm formation once the concentration was below the minimum inhibitory concentration (MIC), SA6(2)

OD - optical density;

Statistical analysis of the results

Since the MIC values of both samples are identical for all five bacterial strains, statistical analysis was not conducted. Also, since the planktonic growth was consistently observed in all samples below the MIC, no statistical analysis was performed. Since two cranberry samples have been tested for total PAC content, an Independent T-test was performed to interpret the differences in results. It was shown that the difference in PAC content was significant ($p < 0.001$). Furthermore, Welch's test was performed, which indicated that the difference was statistically significant ($p = 0.002$).

Using the Paired Samples T-test, it has been observed that there was no statistical significance in OD values between two *E coli* strains for cranberry sample 1 used in the analysis (Student's $t = -0.276$, $df = 9$, $p = 0.789$).

For all three strains of *S aureus*, when the concentration of the sample 1 has dropped below MIC, absorbance couldn't be read by the instrument within the range of concentrations of 1000 µg/mL – 1.95 µg/mL (Table 14) because of the overflow. Therefore, Friedman's test has been used to assess statistical significance for sample 1 within the range of concentrations of 0.975 µg/mL – 0.0005 µg/ for the mentioned strains.

Table 24: Friedman test followed by Durbin-Conover test (cranberry sample 1 tested on 3 strains of *S aureus* within mentioned range of concentration)

ANOVA (Non parametric)	Statistic	p-value
OD <i>S aureus</i> ATCC 6538 - OD <i>S aureus</i> ATCC 25923	3.67	0.001
OD <i>S aureus</i> ATCC 6538 - OD <i>S aureus</i> NCTC 12393	4.90	< 0.001
OD <i>S aureus</i> ATCC 25923 - OD <i>S aureus</i> NCTC 12393	8.57	< 0.001

Table 25: Friedman test followed by Durbin-Conover test (cranberry sample 2 tested on 3 strains of *S aureus* within mentioned range of concentration)

Pairwise comparisons (Durbin-Conover)	Statistic	p-value
OD <i>S aureus</i> NCTC 12393 - <i>S aureus</i> ATCC 25923	4.28	< 0.001
OD <i>S aureus</i> NCTC 12393 - <i>S aureus</i> ATCC 6538	1.34	0.195
<i>S aureus</i> ATCC 25923 - <i>S aureus</i> ATCC 6538	2.94	0.008

Results of the test indicated a strong difference between the groups being compared ($\chi^2 = 18.5$, $df = 2$, $p < 0.001$). The pairwise comparisons using the Durbin-Conover test indicated that all three strains had significantly different OD values (Table 24).

Paired sample T-test for cranberry sample 2 had the purpose to demonstrate if there was a statistical significance in OD results when two *E coli* strains have been tested with the solution of sample 2 within the range of concentration of 1000 $\mu\text{g/mL}$ – 1.95 $\mu\text{g/mL}$.

Using the Paired Samples T-test it has been observed that there was no statistical significance in OD values between two *E coli* strains for cranberry sample 2 used in the analysis ($t = 1.6$, $df = 9$, $p = 0.129$). The results were consistent with the results from the paired sample T-test of sample 1.

For all three strains of *S aureus*, when the concentration of the sample 2 had dropped below MIC, absorbance couldn't be read by the instrument within the range of concentrations of 1000 $\mu\text{g/mL}$ – 1.95 $\mu\text{g/mL}$ because of the overflow. Therefore, One-way ANOVA with repeated measures had been used to assess statistical significance for sample 1 within the range of concentrations of 0.975 $\mu\text{g/mL}$ – 0.0005 $\mu\text{g/mL}$ for the mentioned strains.

The results $\chi^2 = 11.2$ and $p = 0.004$ indicated statistical difference in OD of sample 2 amongst different strains of *S aureus*. Durbin-Conover test has shown there was a significant difference between *S aureus* NCTC 12393 and *S aureus* ATCC

25923 ($p < 0.001$). There was no significant difference between *S aureus* NCTC 12393 and *S aureus* ATCC 6538 ($p = 0.195$). Also, there was a significant difference between *S aureus* ATCC 25923 and *S aureus* ATCC 6538 ($p = 0.008$) (Table 25).

Discussions

In this study, two commercially available dry cranberry extracts were used to treat two strains of Gram-negative bacteria *E coli* and three strains of Gram-positive bacteria, *S aureus*. HPLC method developed by Brown and Shipley was used to determine whether the samples possess anthocyanins characteristic for the cranberry profile, featuring: peonidin-3-O-galactoside (P3Ga), cyanidin-3-O-galactoside (C3Ga), cyanidin-3-O-arabinoside (C3Ar), peonidin-3-O-arabinoside (P3Ar) and smaller amounts of cyanidin-3-O-glucoside (C3Gl) and petunidin-3-O-galactoside.¹³

Other methods which could serve as identity confirmation of the cranberry origin,¹⁵ have proposed the following markers: the ratio of epicatechin to catechin, the ratio of procyanidins to anthocyanins and the ratio of procyanidin A2 to the total procyanidin content. These markers and their ratios were then analysed using principal component analysis (PCA) to ensure compliance. It has been found that most cranberries were mostly fabricated with *Morus nigra* and *Hibiscus* extract, which contain mostly cyanidin-glucoside and cyanidin-rutinoside. The used method in the study has shown positive results, so both dry cranberry extracts were indeed derived from cranberry.

PAC content was measured using a modified Bate-Smith method. This method was based on the acid-catalysed cleavage of PAC into a carbocation (representing the extension units) and a terminal flavan-3-ol unit. The reaction was carried out with 95 % (v/v) butanol acidified with 5 % (v/v) HCl. Fe (III) sulphate then catalyses the autooxidation of the carbocation, converting the colourless PAC into red anthocyanidins. The resulting colour change was quantified by measuring the absorbance at approximately 550 nm.

Procyanidin B2 was chosen as the standard instead of the more conventional cyanidin-chloride. Unlike other berries, cranberries are rich in A-type PAC, which contain at least one double linkage consisting of a C-C (sigma) bond and an additional C-O-C (ether) bond. The most common A-type PAC are A1 and A2, with A2 being the predominant form in cranberries.

PAC A is more stable in acidic conditions and when heated because of an additional ether (C2-O-C7) bond. PAC B2 inverts to PAC A2, which then completely oxidises to its respective anthocyanin, while PAC A oxidises entirely. Transformation of procyanidin B-type into A-type happens via abstraction of the hydrogen atom at the C-2 position during radical oxidation.

With this method, the total concentration of PAC is still underestimated, but it is better than the amount calculated by using cyanidin chloride as a standard. If cyanidin chloride was used as a standard, total PAC would be overestimated.

The results indicate statistical significance between total PAC content in two samples ($p < 0.001$), with the cranberry sample 2 having more total PAC content. Both samples have exhibited minimal inhibitory concentrations of the same value, meaning that they do not differentiate in the mentioned attribute. It was also observed that both samples stimulate the planktonic growth of the bacteria. Unexpected results are related to the biofilm formation. It has been shown that both samples stimulate biofilm formation on all strains of bacteria once the concentration is below MIC. Both sample 1 and cranberry sample 2 showed no statistically significant effect on biofilm formation in the two *E coli* strains. Also, in sample 1, statistical significance has been found on biofilm formation in all three *S aureus* strains, while in sample 2, there was no significant difference between *S aureus* NCTC 12393 and *S aureus*

ATCC. On the other hand, sample 2 has shown a statistically significant difference in biofilm formation of *S aureus* ATCC 25923 and *S aureus* ATCC 6538 strains.

Since the cranberry extracts have not been isolated from human urine after consumption, but was rather *in vitro* examined, no factor of human organism could have stimulated the growth of the biofilm. Several factors would contribute to stimulation of biofilm formation *in vivo*, such as toxin alpha-haemolysin (HlyA) which disrupts the epithelium cells that release iron. Iron is considered a uropathogenic *E coli* (UPEC) virulence factor.¹⁶ Once surface cells are destroyed, deeper tissue is exposed to further bacterial infection and biofilm is formed. Also, human urine contains iron that bacteria can utilise via their scavenging systems. However, since the samples of the urine have not been collected, neither of these factors could have induced biofilm formation.

Therefore, it is safe to assume that stimulation of the biofilm formation once the concentration of the samples was below MIC, could be attributed to quorum sensing. Quorum sensing (QS) is responsible for the phenotype change from individual mobile bacteria to stationary intracellular-like microorganisms due to changes in the gene expression, where synthesis of the pili is downregulated and synthesis of proteins and other elements of the biofilm is upregulated.¹⁷

QS is the result of the activity of various small molecules that act as autoinducers. Gram-negative bacteria produce N-acyl homoserine lactones (AHL) that passively diffuse through the cell wall. On the other hand, Gram-positive bacteria produce peptide autoinducers that require active transport via ATP transporters. These molecules are cleared out from the bacteria cells as being produced. Once the bacteria growth hits a plateau, the extracellular concentration of autoinducers increases and eventually hits a threshold, leading to increased intracellular concentration. Inside the cell, autoinducers bind to the receptors and signal cascades that affect transcription factors and, ultimately, gene expression.¹⁸

Autoinducing peptides (AIP) of Gram-positive bacteria bind to a kinase that phosphorylates a transcription factor that regulates gene expression. Another option is that an autoinducing peptide directly binds to a transcription factor.¹⁹ On the other side, Gram-negative bacteria produce

AHL which acts like a signalling molecule that directly binds to the transcription factor.

For *E coli*, quorum sensing is mediated by auto-inducer-2 (AI-2) which synthesis is regulated by *luxL* and *luxM* genes. It can also function as an autoinducer for some Gram-positive bacteria, thus enabling communication with different bacterial species.²⁰

Since cranberry formulations are generally used to treat urinary tract infections (UTI) caused by *E coli* (UPEC), it is found worthwhile to discuss the mechanism by which *E coli* attaches itself to the epithelium of UTI. There are three adhesion mechanisms that allow the adhesion of UPEC to urethral epithelium: P pili, type 1 pili and F9 pili.²¹

Lectin FimH is located at the tip of the pili type 1 and it is able to bind to mannose structures of uroplakin 1a(UPIa) and α 3 and β 1 integrins in healthy epithelium.¹² It is called mannose-sensitive, considering that it binds to glycoproteins in the mannose. These pili enable initial phase of UTI. FimH is expressed at the tip of F9/Yde/Fml pili and it binds to the Gal(β 1-3)GalNAc bearing glycoprotein in inflamed, but not in healthy tissue. PapG is expressed at the tip of P pili and it binds to galabiose (Gal(α 1-4)Gal β glycoproteins. It is responsible for the bacterial colonisation of the upper urinal tract. P pili are called mannose-resistant because, instead of mannose, it binds to the already mentioned galactose disaccharide.

UPEC attachment consequentially triggers actin cytoskeletal reconstruction, which results in the uptake of bacteria by the mechanism of phagocytosis. The cell itself can react to the interfering bacteria via exocytosis, or the bacteria will infiltrate the cytoplasm. Once in the cytoplasm, bacteria can either multiply and fight the natural defences of the cell, or they can remain dormant by binding to the host F-actin filaments and forming quiescent intracellular reservoirs (QIRs).¹²

P pili (*P fimbriae*) is composed of the following proteins: PapA, PapK, PapE, PapF and PapG. PapG protein, found at the top of the P pili, binds to the galactose disaccharide (α -d-galactopyranosyl-(1-4)- β -dgalactopyranoside) located at the surface of urinary epithelium in the upper UT. The binding of PapG to galactose disaccharide causes the release of sphingolipid ceramids which act as agonists of Toll-like receptor 4 (TLR4).¹⁰

Once TLR4 recognises bacterial lipopolysaccharide (LPS), cell immune response is activated. Inflammatory mediators are produced and neutrophils are required. Initial immune response is useful against fighting bacterial infection, but it also damages local tissue and contributes to the development of acute pyelonephritis.

There are three types of PapG proteins: PapGI, II and III. Each of them is specific for different binding site at the galabiose core. PapGII is bound to globotetraosylceramide (GbO4). GbO4 is a glycolipid where the digalactoside core is bound to N-acetyl-galactosamine on one side and to ceramide on the other side.

Pap GII consists of two regions. Region 1 is the C-terminus and it is a pilin domain, while region 2 is the N-terminus which binds to the receptor. Region 1 is a β barrel consisting of b, p, o, c, n, i stands. Region 2 is made of an antiparallel β sheet consisting of e, a, o, g, k and j strands. This central β sheet is surrounded by two double β strands from one side and by an α -helix from another side. Between the strand o and α -helix there is a large loop. Together, this loop and the y, j, g and k strands and the α -helix form the receptor binding site.²²

The mechanism by which the human body tries to stop biofilm formation is related with the Tamm-Horsefall protein. Tamm-Horsefall protein is also known as uromodulin (UMOD). It is a glycoprotein produced solely in the renal cells of the descending Henle loop. Its secretion is a part of the innate immune system. THP is rich in mannose and has affinity to FimH of type 1 pili.

The anti-inflammatory effect of the cranberry (*V macrocarpon*) is attributed to its ability to interfere with signalling molecules involved in the inflammatory response. The basis of anti-inflammatory response is the antioxidative property of cranberry components. Once the extract components interact with redox-sensitive transcription factors of signalling transduction pathways: NF- κ B, 5'-AMP protein kinase, MAPK and JNK.

Study of Hannon and others suggests that cranberry extracts decreased the activity of NF- κ B, MAPK and nuclear factor of activated T cells (NFAT), while in higher concentration, cranberry extract stimulates JNK, MAPK and p38.²³ Without further molecular research, it is not clear how the cranberry sample induces biofilm formation

when the concentration is below MIC. However, it is safe to assume that the environmental stress due to dilution of the samples of bacteria, at one point, activates *luxS* and *luxG* genes, which further induce synthesis of autoinducer-2 (AI-2), which enables biofilm formation.

On the other hand, urinary infections caused by *S aureus* are relatively uncommon and can happen in the hospital surroundings, in cases when patients have inserted a catheter in the urinary tract or some other instrumentation. *S aureus* can ascend the urinary tract when the patient is under anaesthesia or has a catheter. It causes complicated urinary infections, especially in diabetic and immunosuppressed patients.²⁴

The results of the study imply that the effect on biofilm formation of the sample is greater in *S aureus* strains rather than in *E coli*. Also, possible explanations of why there are such variations in optical density (OD) readings between strains, even when they are present at the same nominal concentration, could be related to cell morphology and size, cell wall composition or lack of it, pigment production and metabolic byproducts and different states of growth. Strains might differ in their dimensions, leading to larger or more irregularly shaped cells scattering light differently, which causes higher or lower OD readings even when the cell numbers are identical. Also, some strains might form clusters which increases light scattering, resulting in higher OD values compared to those cells that remain single. Differences in peptidoglycan thickness of *S aureus* strains or variations in cell surface proteins can change the refractive index of the cells, leading to lower or higher optical density. Some strains produce more extracellular polymeric substances or express different surface adhesins. These molecules can affect light scattering and absorption, impacting the OD measurement. Differences in OD values could have a connection with the sample itself, that is red colour. Even diluted, some pigments may absorb light and increase OD values.

However, it is more precise to postulate that the variation of metabolic activity has led to differences in the concentration of intracellular or extracellular compounds that absorb light. Even at the same concentration, if the cells are at different growth stages, their internal composition and refractive properties might differ. For instance, cells in the stationary phase might have a thicker

cell wall or different internal storage compounds compared to those in the logarithmic phase, altering their optical properties.

The found results of significant differences between *S aureus* NCTC 12393 vs *S aureus* ATCC 25923 and *S aureus* ATCC 25923 vs *S aureus* ATCC 6538 ($p < 0.001$ and $p = 0.008$, respectively) suggest that these strains likely have inherent differences in one or more factors mentioned above. The non-significant difference between *S aureus* NCTC 12393 and *S aureus* ATCC 6538 implies that these two strains have more similar physical or biochemical properties affecting their OD measurements, even though they are distinct strains.

Conclusion

This study demonstrated that commercially available cranberry extracts, confirmed to be authentic *Vaccinium macrocarpon* products by HPLC anthocyanin profiling, possess significant antimicrobial properties against both Gram-negative and Gram-positive bacteria. Both extracts exhibited comparable minimum inhibitory concentrations (MICs) against *Escherichia coli* strains (125 µg/mL) and *Staphylococcus aureus* strains (250 µg/mL), affirming their potential as natural antibacterial agents. The quantification of total proanthocyanidin (PAC) content using a modified Bate-Smith method revealed that differences in PAC levels between the extracts were statistically significant. Despite these differences, the MIC values remained consistent, suggesting that while the overall PAC content may vary, the bioactive components responsible for antibacterial effects are present in effective concentrations in both samples.

A particularly noteworthy finding is the dual behaviour observed at sub-inhibitory concentrations. Although both extracts effectively inhibit bacterial growth at concentrations above the MIC, lower doses were found to stimulate planktonic growth and, more critically, enhance biofilm formation. This paradoxical effect is likely linked to quorum sensing mechanisms, where environmental stress induced by sub-MIC levels triggers bacteria to upregulate biofilm-associated genes. The enhanced biofilm formation poses a potential challenge

for therapeutic applications, as biofilms are known to increase bacterial resistance to antimicrobial agents.

Statistical analyses, including independent T-tests and non-parametric Friedman tests, confirmed significant differences in biofilm formation across various strains, particularly among *S aureus* isolates. Variations in optical density measurements suggest that intrinsic factors such as cell morphology, surface protein expression and metabolic state may influence bacterial responses to cranberry extract treatment. These findings underscore the complexity of bacterial adaptation and the need for careful consideration of dosage in clinical applications.

In summary, this study not only validates the antimicrobial efficacy of cranberry extracts but also highlights the nuanced effects these natural products can have on bacterial behaviour. While the inhibitory effects at or above MIC levels are promising for combating infections—especially urinary tract infections commonly caused by *E coli*—the stimulation of biofilm formation at lower concentrations warrants further investigation. Future research should focus on elucidating the molecular pathways underlying this biofilm induction and optimising extract formulations to enhance antibacterial action while mitigating unintended stimulation of biofilm formation.

Overall, the findings provide a robust framework for future studies aimed at harnessing the therapeutic potential of cranberry extracts. By carefully balancing the effective antimicrobial properties with the observed biofilm-inducing effects at sub-MIC levels, cranberry-derived compounds could be optimised for use as both preventive and therapeutic agents against biofilm-associated infections.

Ethics

This study did not directly involve with human participants or experimental animals. Therefore, the ethics approval was not required in this paper.

Acknowledgement

None.

Conflicts of interest

The authors declare that there is no conflict of interest.

Funding

The determination of total proanthocyanidin (PAC) content in the purchased samples was supported by *Amsal Pharmaceuticals d.o.o.* Sarajevo, which provided laboratory equipment and analytical standards. HPLC instrumentation, chemicals and standards were provided by International Burch University of Sarajevo. All microbiological equipment and analyses were also conducted at International Burch University. No additional external funding was received for this study.

Data access

The data that support the findings of this study are available from the corresponding author upon reasonable individual request.

Author ORCID numbers

Anisa Veledar-Hamalukić (AVH):
0009-0004-0417-3424
Monia Avdić (MA):
0000-0001-5457-6900
Amra Demirović (AD):
0009-0008-9749-783X

Author contributions

Conceptualisation: AVH, MA
Methodology: AVH, MA
Validation: MA
Formal analysis: AVH, AD
Investigation: AVH, AD

Data curation: AVH, AD
 Writing - original draft: AVH
 Writing - review and editing: AVH, MA, AD
 Supervision: MA
 Project administration: MA
 Funding acquisition: None.

References

1. Di Martino P. Extracellular polymeric substances, a key element in understanding biofilm phenotype. *AIMS Microbiol.* 2018;4(2):274–88. doi: 10.3934/microbiol.2018.2.274.
2. Petrova OE, Sauer K. Sticky situations: key components that control bacterial surface attachment. *J Bacteriol.* 2012 May 15;194(10):2413–25. doi: 10.1128/JB.00003-12.
3. Zheng S, Bawazir M, Dhall A, Kim HE, He L, Heo J, et al. Implication of surface properties, bacterial motility, and hydrodynamic conditions on bacterial surface sensing and their initial adhesion. *Front Bioeng Biotechnol.* 2021 Feb 12;9:643722. doi: 10.3389/fbioe.2021.643722.
4. Sharma S, Mohler J, Mahajan SD, Schwartz SA, Bruggemann L, Aalink R. Microbial biofilm: a review on formation, infection, antibiotic resistance, control measures, and innovative treatment. *Microorganisms.* 2023 Jun 19;11(6):1614. doi: 10.3390/microorganisms11061614.
5. Sauer K, Stoodley P, Goeres DM, Hall-Stoodley L, Burmølle M, Stewart PS, et al. The biofilm life cycle: expanding the conceptual model of biofilm formation. *Nat Rev Microbiol.* 2022 Oct;20(10):608–20. doi: 10.1038/s41579-022-00767-0.
6. Zhang L, Jin M, Sun M. Inhibition characteristics of biofilm structure of *Staphylococcus aureus*. *Cell Mol Biol.* 2020 May 16;66(2):204–11. doi: 10.14715/cmb/2020.66.2.32.
7. Detho H. Biofilm formation and antibiotic resistance in uropathogenic *Escherichia coli*: The quest for effective treatment of urinary tract infections. *Pure Appl Biol.* 2024 Mar 10;13(1). doi: 10.19045/bspab.2024.130004.
8. Sauer MM, Jakob RP, Eras J, Baday S, Eriş D, Navarra G, et al. Catch-bond mechanism of the bacterial adhesin FimH. *Nat Commun.* 2016 Mar 7;7(1):10738. doi: 10.1038/ncomms10738.
9. Kostakioti M, Hadjifrangiskou M, Hultgren SJ. Bacterial biofilms: development, dispersal, and therapeutic strategies in the dawn of the postantibiotic era. *Cold Spring Harb Perspect Med.* 2013 Apr 1;3(4):a010306–a010306. doi: 10.1101/cshperspect.a010306.
10. Ribić R, Meštrović T, Neuberg M, Kozina G. Effective anti-adhesives of uropathogenic *Escherichia coli*. *Acta Pharm.* 2018 Mar 1;68(1):1–18. doi: 10.2478/acph-2018-0004.
11. Vasudevan S, Thamil Selvan G, Bhaskaran S, Hari N, Solomon AP. Reciprocal cooperation of type A procyanidin and nitrofurantoin against multi-drug resistant (MDR) UPEC: A pH-dependent study. *Front Cell Infect Microbiol.* 2020 Aug 11;10:421. doi: 10.3389/fcimb.2020.00421.
12. Maximilian Matthias Sauer. Catch and release: mechanism and binding epitope of the bacterial adhesin fimh. Institute of Molecular Biology and Biophysics, ETH Zurich, Switzerland; 2017.
13. Brown PN, Shipley PR. Determination of anthocyanins in cranberry fruit and cranberry fruit products by high-performance liquid chromatography with ultraviolet detection: single-laboratory validation. *J AOAC Int.* 2011;94(2):459–66. PMID: 21563679.
14. Avdić M, Džuzić N, Hasanić O, Spahić A, Smajlović Skenderagić L, Badnjević A, et al. Development of a novel biofilm classification tool and comparative analysis of result interpretation methodologies for the evaluation of biofilm forming capacity of bacteria using tissue culture plate method. *Med Glas.* 2018 Aug 24;16(1):7–12. doi: 10.17392/997-19.
15. Gardana C, Scialpi A, Fachechi C, Simonetti P. Identification of markers for the authentication of cranberry extract and cranberry-based food supplements. *Heliyon.* 2020 Apr;6(4):e03863. doi: 10.1016/j.heliyon.2020.e03863.
16. Whelan S, Lucey B, Finn K. Uropathogenic *Escherichia coli* (UPEC)-Associated urinary tract infections: the molecular basis for challenges to effective treatment. *Microorganisms.* 2023 Aug 28;11(9):2169. doi: 10.3390/microorganisms11092169.
17. Harmsen M, Yang L, Pamp SJ, Tolker-Nielsen T. An update on *Pseudomonas aeruginosa* biofilm formation, tolerance, and dispersal. *FEMS Immunol Med Microbiol.* 2010 Aug;59(3):253–68. doi: 10.1111/j.1574-695X.2010.00690.x.
18. Parsek MR, Greenberg EP. Acyl-homoserine lactone quorum sensing in gram-negative bacteria: a signaling mechanism involved in associations with higher organisms. *Proc Natl Acad Sci U S A.* 2000 Aug 1;97(16):8789–93. doi: 10.1073/pnas.97.16.8789.
19. Prazdnova EV, Gorovtsov AV, Vasilchenko NG, Kulikov MP, Statsenko VN, Bogdanova AA, et al. Quorum-Sensing Inhibition by Gram-Positive Bacteria. *Microorganisms.* 2022 Feb 3;10(2):350. doi: 10.3390/microorganisms10020350.
20. Kungwani N, Shukla SK, Subba Rao T, Das S. Biofilm-mediated bioremediation of polycyclic aromatic hydrocarbons: current status and future perspectives. In: *Microbial Biodegradation and Bioremediation*. Amsterdam, NA: Elsevier; 2022. p. 547–70. doi: 10.1016/B978-0-323-85455-9.00021-7.
21. Zhou Y, Zhou Z, Zheng L, Gong Z, Li Y, Jin Y, et al. Urinary tract infections caused by uropathogenic *Escherichia coli*: mechanisms of infection and treatment options. *Int J Mol Sci.* 2023 Jun 23;24(13):10537. doi: 10.3390/ijms241310537.
22. Dodson KW, Pinkner JS, Rose T, Magnusson G, Hultgren SJ, Waksman G. Structural Basis of the interaction of the pyelonephritic *E. coli* adhesin to its human kidney receptor. *Cell.* 2001 Jun 15;105(6):733–43. doi: 10.1016/S0092-8674(01)00388-9.
23. Hannon DB, Thompson JT, Khoo C, Juturu V, Vanden Heuvel JP. Effects of cranberry extracts on gene expression in THP -1 cells. *Food Sci Nutr.* 2017 Jan;5(1):148–59. doi: 10.1002/fsn3.374.
24. Xu K, Wang Y, Jian Y, Chen T, Liu Q, Wang H, et al. *Staphylococcus aureus* ST1 promotes persistent urinary tract infection by highly expressing the urease. *Front Microbiol.* 2023 Feb 22;14:1101754. doi: 10.3389/fmicb.2023.1101754.